Transition state structure invariance to model system size and calculation levels: A QM/MM study of the carboxylation step catalyzed by Rubisco

ARTICLE *in* THEORETICAL CHEMISTRY ACCOUNTS · FEBRUARY 1999

Impact Factor: 2.23 · DOI: 10.1007/s002140050434

5 AUTHORS, INCLUDING:

Vicente Moliner
Universitat Jaume I
164 PUBLICATIONS **2,578** CITATIONS
SEE PROFILE

Vicent S Safont
Universitat Jaume I
84 PUBLICATIONS **1,423** CITATIONS
SEE PROFILE

Orlando Tapia
Uppsala University
236 PUBLICATIONS **4,265** CITATIONS
SEE PROFILE

Theor Chem Acc (1999) 101:228–233
DOI 10.1007/s00214980m117

Theoretical
Chemistry Accounts

Regular article

Transition state structure invariance to model system size and calculation levels: a QM/MM study of the carboxylation step catalyzed by Rubisco*

V. Moliner[1], **J. Andrés**[1], **M. Oliva**[1], **V.S. Safont**[1], **O. Tapia**[2]

[1] Department of Experimental Sciences, University Jaume I, Box 224, E-12080 Castelló, Spain
[2] Department of Physical Chemistry, Uppsala University, Box 532, S-75121 Uppsala, Sweden

Received: 24 March 1998 / Accepted: 3 September 1998 / Published online: 10 December 1998

Abstract. The present study elucidates structural features related to the molecular mechanism in the carboxylation step of the reaction catalyzed by Rubisco. Starting from the initial X-ray Protein Data Bank structure of a Rubisco monomer, the reactive subsystem in vacuo is subjected to quantum chemical semiempirical and ab initio studies, while the effects of the protein environments are included by means of a hybrid quantum mechanical/molecular mechanical (QM/MM) approach. The QM/MM is used to characterize the transition structure for carboxylation inside the protein. The calculations were made with the AM1/CHARMM/GRACE scheme. Comparisons between the in vacuo and in situ transition structures show remarkable invariance with respect to geometric parameters, index and transition vector amplitudes. The transition state couples the carbon dioxide attack to the C2 center of the substrate in its dienol form with a simultaneous intramolecular hydrogen transfer from the C2 atom to the hydroxyl group linked to the C3 center. This study suggests that carboxylation may be simultaneously coupled to the activation of the C3 center in the enzyme.

Key words: Rubisco – Carboxylation step – QM/MM – Hybrid theoretical calculations – Transition state structure

1 Introduction

The understanding at an electronic/molecular level of reaction mechanisms requires a detailed knowledge of the transition structures. The characterization of such stationary points, for a given chemical interconversion process, permits a fairly clear representation of possible molecular mechanisms [1–4]. Theoretically, there has been a shift in perception about the nature of the transition structure. This perception has moved from the early concept of an unstable molecular configuration [5, 6] to the presence of a real molecule characterized with energy levels having finite lifetimes and a well-defined geometry obtained as a saddle point of index one [7]. From catalytic antibodies [8–13], via the spectroscopy of the transition state [14–16], to the concept of transition state analogs [17, 18], the idea of a real, existing structure [1, 19–22] is gaining support, and beyond being a theoretical hypothesis it is becoming an experimentally documented fact. The saddle points of index one [23–25] sustaining vibrational-rotational (librational) quantum states will be referred to as transition state structures (TSSs).

The TSSs of a number of reactions in vacuo have shown to be fairly invariant with respect to the choice of the molecular model as well as the level of theory employed [3, 26–35]. The geometric parameters and the amplitudes of the transition vector are found to be fairly well defined. However, environmental effects should affect these quantities [36–38] and in fact, methods developed to study chemical reactions in condensed phases [36, 39–44] or in a protein medium [37, 38, 45–52] have demonstrated this to be true. It is therefore necessary to establish whether or not a full representation of protein core effects [38] would change the property of invariance detected for TSS in small molecular models in vacuo.

In this paper we use combined quantum mechanical (QM) methods and molecular mechanical (MM) force fields to explore the carboxylation process catalyzed by the enzyme Rubisco. These hybrid models treat the reacting system (or the active site in an enzyme) explicitly by a QM method, while the environmental molecules (or amino acids) are approximated by a standard MM force field. The TSS has been located and characterized with AM1/CHARMM calculations involving a fully flexible active-site region by means of a novel procedure (GRACE) [52, 53] developed by Williams and co-

* Contribution to the Proceedings of Computational Chemistry and the Living World, April 20–24 1998, Chambery, France

Correspondence to: V. Moliner

workers. The results have been compared with those obtained in vacuo using sophisticated computational levels and two different substrate models. A discussion of the system embedded in the enzyme allows for a detailed analysis of the active-site residues effects and the invariance of the TSS to the level of computational theory and the size of the molecular model.

1.1 Rubisco enzyme

Rubisco catalyzes several chemically distinct reactions. From the carboxylation of RuBP (D-ribulose 1,5-bisphosphate) to the production of two molecules of 3-phospho-D-glycerate (PGA), the catalytic reaction involves different steps, some of which can occur as partial reactions forming intermediates [54]. The commonly accepted reaction steps for carboxylation of RuBP [55, 56] are depicted in Fig. 1. The overall reaction can be dissected into a series of consecutive steps: enolization, carbon dioxide fixation, hydration, C2—C3 bond breaking and inversion of the configuration at the C2 center [55–57]. Enolization is the first and possibly rate limiting step [58–65] prompting intermediate I, submitted to a C2 carboxylation via an electrophilic attack of CO_2, to form II. Hydration of this C3 ketone intermediate (II) leads to a gem-diol III. Deprotonations of the hydroxyl oxygen atoms at the C3 center initiates C2—C3 bond cleavage. Following this bond breaking process, one molecule of PGA (IV) is formed together with the aci-acid species (V). A stereospecific protonation at the C2 center is required to obtain the second PGA (VI). We have theoretically documented this mechanism using in vacuo models [66].

Theoretical mechanistic studies on a number of issues related to the unusual catalytic behavior of Rubisco have already been reported. In particular, TSSs were calculated in vacuo for the initial step in carboxylation, oxygenation, as well as intramolecular hydrogen transfer leading to enolization and self-inhibitory pathways [31, 34, 66–71]. These self-inhibitory pathways can be attained by means of intramolecular retroenolizations leading to several inhibitors: D-xylulose 1,5 bisphosphate, D-arabinitol 1,5 bisphosphate, and D-ribitol 1,5 bisphosphate [71]. These results show very similar geometries for TSS and an invariance with respect to the components of the transition vector representing the fluctuation patterns at this point. It is not known whether the mechanistic steps obtained in this manner are compatible with the presence of the protein. This is an important challenge and, to approach this fundamental issue, we have selected the only step for which an experimentally characterized transition state analog has been determined: the carboxylation step [72]. This has already allowed us to compare experimental results with in vacuo theoretical TSS using quite simple molecular models [31, 34, 66, 67, 70].

Fig. 1. Proposed reaction pathway for the carboxylation of RuBP catalyzed by Rubisco, extracted and modified from Hartman and Harpel [56]

2 Models and computing methods

Substantial insight into the structure and mechanism of Rubisco enzyme has come from crystallographic investigations [65, 73–76]. The starting point for our calculations was the 1.6 Å resolution structure of the ternary complex (Protein Data Bank code 8RUC). For meaningful calculations to be performed, it is essential to have a high-resolution structure, and that it accurately represent the enzyme-substrate complex.

For the hybrid QM/MM calculation, owing to the great size of tetrameric Rubisco molecules, and because of the independence of the subunits, only one subunit of them was considered. Hydrogens were added, with all ionizable groups set at a state complementary to pH 7.

The entire simulation system was divided in QM and MM regions. After some experimentation with different partitioning schemes, it was decided to treat the substrate RuBP and the carbon dioxide molecule quantum mechanically, while the rest of the protein and the water molecules were treated classically. This is not a serious drawback. We have checked the invariance of the TSS when the magnesium coordination sphere is treated quantum mechanically. These calculations were carried out using two molecular systems: model I, a five-carbon framework (3,4-dihydroxy-2-pentanone) treated at an AM1 level; and model II, the same five-carbon system with the magnesium coordinate sphere now treated ab initio with a 3-21G basis set. The TSSs were carefully characterized. At each point, the Berny analytical gradient optimization routines were used [77, 78]. The requested convergence on the density matrix was 10^{-9} atomic units; the threshold value of maximum displacement was 0.0018 Å and that of the maximum force was 0.00045 hartree/bohr. The nature of each stationary point was established by calculating analytically and diagonalizing the

Hessian matrix. All these calculations were carried out using the GAUSSIAN 94 program [79].

In Fig. 2, model I corresponds to the QM atoms (pink region) and for model II the side chain rest of the Lys-201 (carbamylated), Asp-203 and Glu-204 residues have been replaced by H atoms. Since we do not yet have reliable AM1 parameters for magnesium, the full coordination sphere was left out the QM system. The QM region, consisting of 29 atoms (pink region of Fig. 2), was chosen as the best compromise between the requirement to represent the reaction region accurately and the need to minimize the number of QM atoms to keep the calculations within reasonable bounds.

Even for such hybrid methodology, computational limitations made it impractical to include the entire protein in the calculations; hence a smaller representative region around the active site was considered. It is important that this simulation zone be large enough to incorporate all residues likely to have a significant effect on the reaction or required for substrate binding. After several tests, a system formed by all residues with an atom within a distance of 18 Å from the Mg atom was selected (Fig. 2). The remaining atoms were deleted.

Once the system was centered about Ng, a solvent boundary potential on the MM water molecules was applied in order to maintain the structure of the water at the edges. The resulting molecular system was a pseudo-sphere of a total of 3525 atoms – active site, bulk protein and crystal water molecules altogether.

Harmonic constraints were also applied to the heavy atoms further than 18 Å away from origin (ca. 500 atoms), that is, a restoring force proportional to the displacement from its initial position was applied to each of these atoms [80]. This serves to preserve the structure of the enzyme, especially where there may be loops of protein disconnected from the main chain because of the truncation.

Once the system was prepared, the hybrid QM/MM optimizations were carried out, where the QM atoms of the reacting system were treated by the AM1 semiempirical molecular orbital method [81] and the MM atoms were minimized by means of the Adopted Basis Newton-Raphson (ABNR) minimization algorithm. The CHARMM24 program [82] was used for all the QM/MM optimizations.

As explained in previous sections, the theoretical description of the main chemical processes that take place in the active site of Rubisco requires a complete characterization of the stationary points. For this purpose, several internal coordinates were fixed at each point and all other degrees of freedom, for each point, were submitted for QM/MM optimization by means of the CHARMM24 program.

Once the quadratic zone was obtained, the new GRACE [52, 53] software was used to refine and characterize QM/MM saddle points of index one using an eigenvalue followed (EF) algorithm. A partial-rational-function-operator/ABNR method was employed, utilizing a Hessian matrix of order 87×87 that describes the curvature of the QM/MM energy hypersurface for the QM-29 atom subset, together with a diagonal Hessian. Then the rest of the system is updated. The r.m.s. residual gradient for the total molecular system is less than 0.005 kcal mol^{-1} $Å^{-1}$ in the optimized structures; these residual gradients are lower than the commonly accepted convergence criteria for optimized geometries of small molecules in quantum chemistry.

We started with a molecular structure selected from the quadratic region of the potential energy surface obtained with CHARMM. In order to demonstrate conclusively that the reported saddle structure was indeed a TSS for the chosen reaction, the path of the intrinsic reaction coordinate was traced from the putative TSS in each direction, leading to the expected reactant- and product-like structures. Finally, the vibrational frequencies of the TSS were determined.

3 Results and discussion

In the QM/MM approach used here, it is not necessary to calculate the potential energy hypersurface in the neighborhood of the TSS since that is described by the normal modes obtained from the diagonalization of the mass-weighted Hessian. The idea of a minimal molecular model and an active control subspace [34, 83] have helped in studying a number of complex reactions in which chemical conversion primarily involves a subset of chemical functions with manageable molecular mod-

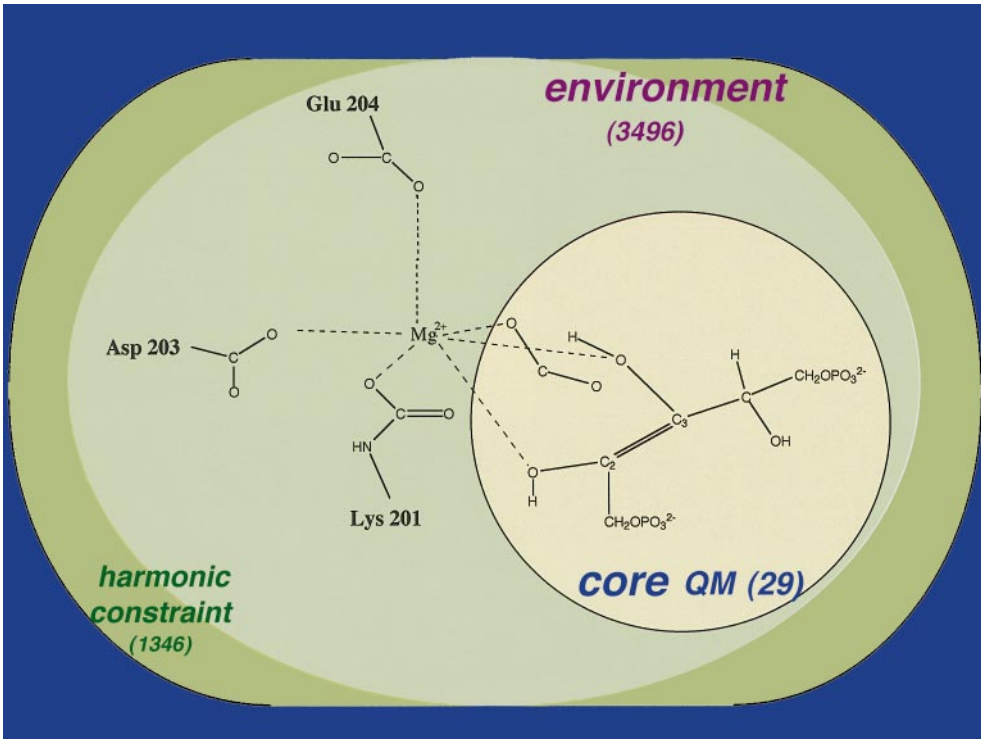

Fig. 2. Schematic representation of the Rubisco active site: the *pink* region corresponds to the QM atoms used in the QM/MM calculations. The numbers of atoms included in the calculation are given in parentheses

els. This principle was used to examine TSSs for the carboxylation mechanism in five-carbon and three-carbon models [31, 34, 66, 67, 70]. Here, the invariance of the transition structures with respect to the level of electronic theory and the size of the control space are examined.

The TSSs found with molecular models I and II for the carboxylation process are depicted in Fig. 3a and b. The geometric details are given in the figure. They give an overview of the global progress, starting from the model substrate in its enediol form, and ending with the carboxylated moiety.

There are several implications to these results: We have been able to describe the carboxylation step with a self-contained molecular model, without calling for external acid-base groups, as is commonly accepted for this and other steps of the Rubisco reaction mechanism [76, 84]. By excluding the protein environment we have shown that the reaction mechanism may be independent of such interactions, at least as far as the geometry of the stationary points is concerned. By modelling the calculated TSS geometries into the active site of Rubisco one can sense the moulding work achieved by the enzyme and, most importantly, to gauge possible roles of actual catalysis for the intermediate steps. The geometric overlap between the carboxylation TSS and the transition state analog CABP (2-carboxy-D-arabinitol-1,5-bisphosphate) is a hint of the relevance that the present theoretical study in vacuo may have for the real system.

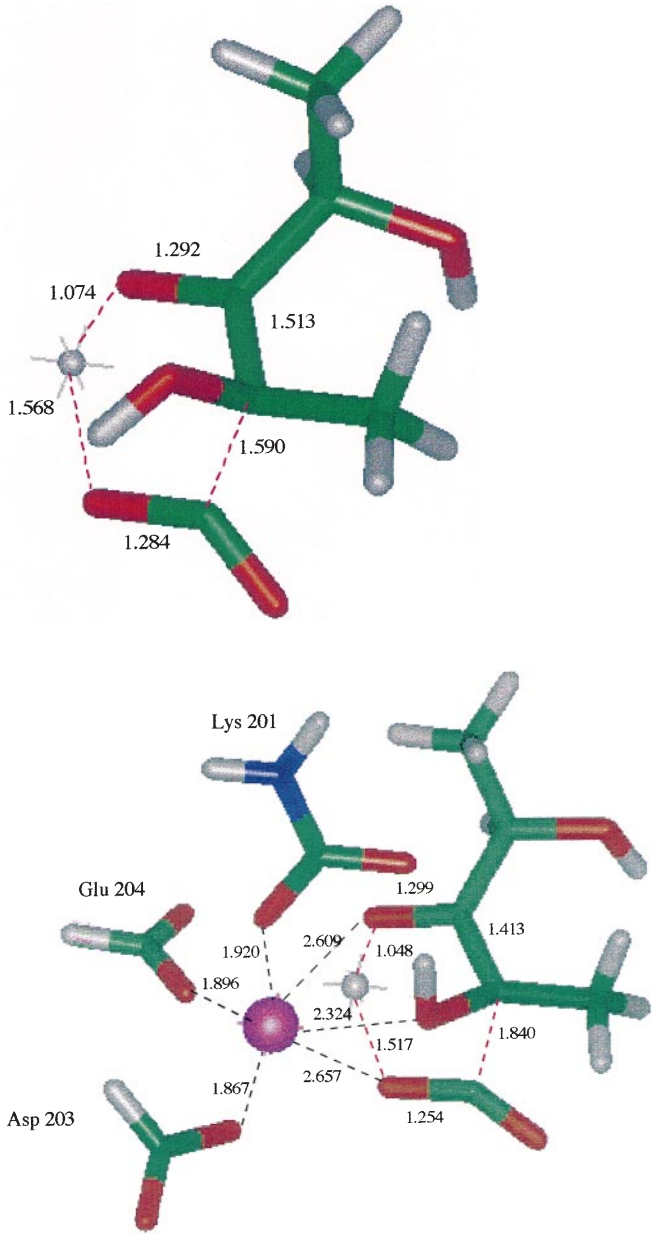

Fig. 3a, b. The TSS for the carboxylation step. **a** Model I, **b** model II [Å]

There is a significant difference between this system and our previously reported carboxylation TSSs [31, 34, 67]. The carboxylation TSSs couple carbon dioxide attack to the C2 center of the substrate in its dienol form with a synchronous interconversion of the C3 hydroxyl into a ketone group. This results in a neutral carboxylic acid moiety with an active carbonyl function at C3. The carbonyl group at C3 is ready to undergo the hydration process that would lead to the gem-diol as we recently reported for the 3-C model [66]. The inclusion of the coordination shell leads to nearly the same TSSs (Fig. 3a, b). Note that the Mg ligand distances cluster in two groups. Those representing side chains are shorter than those corresponding to the substrate atoms. The former are located in one hemisphere, the latter have enough space to allow reactive events.

A key issue now is to test whether the presence of the protein would allow for interconversion at the active site. The QM/MM TSS obtained is depicted in Fig. 4. The saddle point for carboxylation was obtained with the full system.

The transition vector of the QM/MM TSS coincides with those obtained for the systems reported in Fig. 3. The proton transfer appears coupled to the carbon dioxide attack at C2 as in the examples in Fig. 3. Again, the coordination sphere to Mg is clearly divided into two hemispheres. The residues Lys 201 (carbamylated), Glu 204 and Asp 203 can be seen to the left of the reactive motif. Even the hydrogen flying in between the C3 hydroxyl and the carbon dioxide appears without any impediment from the Mg or any other residue. This point is suggestive.

The frequencies of the normal modes show an interesting trend. From the simple model in vacuo to the complete protein surroundings, the force constants become smaller. The coordination shell seems to help the system in softening the vibrational degrees of freedom. Nevertheless if we look at the imaginary frequencies we obtain for the structure in Fig. 3a, 741.9i; for that in Fig. 3b, 741.4i; and for the geometry in Fig. 4 we get 1090.1i. The AM1 calculation for the model in vacuo reproduces well the ab initio figure. The effect of the protein environment is to keep a big amount of small frequencies associated with breathing movements of the protein. We can consider that the complex system helps to soften the fluctuations at the active site, while it keeps the geometry and transition vector amplitudes, invariant.

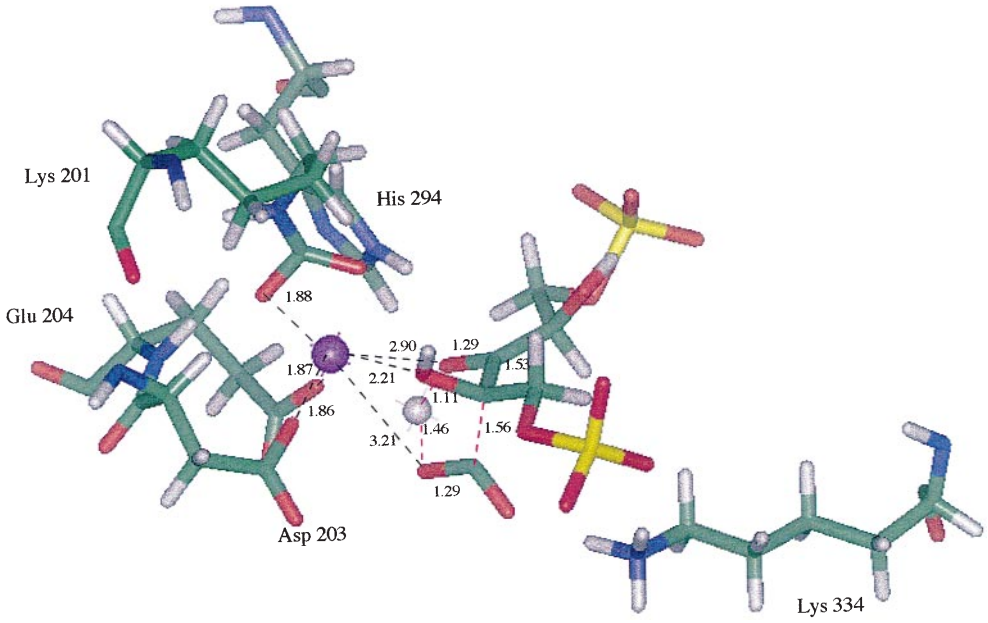

Fig. 4. QM/MM TSS refined using AM1/CHARMM/GRACE for the Rubisco carboxylation step. [Å]

It is interesting to compare the role of the carboxyl group from the carbamylated Lys 201 in the ab initio and QM/MM calculations. The hydroxyl hydrogen at C2 makes a hydrogen bond with one oxygen in both cases. Normal mode animation shows these atoms with negligible fluctuations, all the action occurs on the chemically active atoms. It seems then that carbamylation influences the reactive subsystem not only by its contribution to the coordination of magnesium at the right place, but also by cooperating with hydrogen bonding to atoms belonging to the complementary space.

In the QM/MM study, the role of Lys 334 confirms the static structural analysis. It is steering the carbon dioxide oxygen. Incidentally, in the oxygenation reaction it may play a similar role.

It has been suggested that His 294 (in Fig. 4) may act as a proton acceptor during tautomerization [76]. The orientation obtained for the saddle point structure is not favorable to make such a contact of course. Our calculations predict that a mutation of this residue may not drastically affect the reaction mechanism as far as intramolecular hydrogen reshuffling is concerned. Here is an issue to be resolved by experiments.

When the geometry of the TSSs is used to replace CABP, [65], no steric hindrances are observed. In addition, the TSSs of the present scheme show great similarities. This ensures surface complementarity between the protein active site and the activated complex of the reaction catalyzed by the enzyme. This study shows that the transition structure and moulded intermediates found here offer a reasonable alternative mechanistic path for the carboxylation chemistry in Rubisco. The bottom line is, as stated in Pauling's lemma [85], that substrate moulding into geometries compatible with the transition structures is essential to allow catalytic activity [3, 7, 33]. Failing to mold may fully prevent the reaction.

4 Final remark

Three transition structures have been characterized via two molecular models in vacuo that share those chemical functional group of D-ribulose-1,5-bisphosphate that are the most important in the carboxylation process catalyzed by Rubisco. Following the intrinsic reaction coordinate path [86] for the three structures back toward reactants or forward to products the TSSs lead from the substrate to the dienol form and thereafter to an acid intermediate. This conclusively demonstrates that the reported structures for carboxylation are indeed a TSS, for the correct reaction. The TSSs appear to be robust entities whose essential structural features are invariant with respect to the nature of their environment.

Acknowledgements. This work was supported by research funds of the DGICYT Dirección General de Investigación, Ciencia y Technologia, (projects PB93-0661 and PB96-0795-C02-02). Calculations were performed on an IBM RS6000 workstation of the Departament de Ciències Experimentals and on two Silicon Graphics Power Challenger L of the Servei d'Informàtica of the Universitat Jaume I. We are indebted to these centers for providing us with computer capabilities. M.O. thanks the Ministerio de Educación y Ciencia for a FPI Formación del Personal Investigator fellowship. O.T. thanks NFR Swedish Research Council for financial support.

References

1. Houk KN, Gustafson SM, Black KA (1992) J Am Chem Soc 114: 8565
2. Williams IH (1993) Chem Soc Rev 277
3. Tapia O, Paulino M, Stamato FMLG (1994) Mol Eng 3: 377
4. Houk KN, González J, Li Y (1995) Acc Chem Res 28: 81
5. Wigner E (1938) Trans Faraday Soc 34: 29
6. Neumark DM (1993) Acc Chem Res 26: 33
7. Tapia O, Andres J, Stamato FMG (1996) In: Solvent effects and chemical reactivity. Kluwer, Dordrecht, pp CF18: 283–361

8. Lerner RL, Tramontano A (1987) Trends Biochem Sci 12: 427
9. Tramontano A, Janda KD, Lerner RA (1988) Science 234: 1566
10. Pollack SJ, Schultz PG (1987) Cold Spring Harbor Symp Quant Biol LII: 97
11. Schultz PG, Lerner RA (1993) Acc Chem Res 26: 391
12. Reymond JL, Jahangiri GK, Stoudt C, Lerner RA (1993) J Am Chem Soc 115: 3909
13. Gouverneur VE, Houk KN, Pascual-Teresa B, Beno B, Janda KD, Lerner RA (1993) Science 262: 204
14. Polanyi JC, Zewail AH (1995) Acc Chem Res 28: 119
15. Neumark DM (1996) Science 272: 1446
16. Wenthold PG, Hrovat DA, Borden WT, Lineberger WC (1996) Science 272: 1456
17. Wolfenden R, Radzicka A (1991) Curr Opin Struct Biol 1: 780
18. Schröer J, Sanner M, Reymond J-L, Lerner RA (1997) J Org Chem 62: 3220
19. Houk KN, Rondan NG, von Rague Schleyer P, Kaufmann E, Clark T (1985) J Am Chem Soc 107: 2821
20. Wu Y-D, Houk KN (1987) J Am Chem Soc 109: 2226
21. Wu Y-D, Houk KN (1987) J Am Chem Soc 109: 906
22. Tapia O, Cárdenas R, Andrés J, Colonna-Cesari F (1988) J Am Chem Soc 110: 4046
23. Mezey PG (1987) Potential energy hypersurfaces. Elsevier, Amsterdam
24. Mezey PG (1980) Theoret Chim Acta 54: 95
25. Mezey PG (1981) In: Computational theoretical organic chemistry. Reidel, Dordrecht, pp 101–128
26. Tapia O, Cárdenas R, Andrés J, Krechl J, Campillo M, Colonna-Cesari F (1991) Int J Quantum Chem 39: 767
27. Tapia O, Jacob O, Colonna F (1992) Theor Chim Acta 82: 217
28. Tapia O, Andrés J, Cárdenas R (1992) Chem Phys Lett 189: 395
29. Tapia O, Jacob O, Colonna F (1993) Theor Chim Acta 85: 217
30. Andres J, Moliner V, Krechl J, Silla E (1994) J Phys Chem 98: 3664
31. Tapia O, Andrés J, Safont VS (1994) J Chem Soc Faraday Trans 90: 2365
32. Andrés J, Moliner V, Safont VS (1995) J Chem Soc Faraday Trans 90: 1703
33. Tapia O, Andres J (1995) J Mol Struct (Theochem) 335: 267
34. Tapia O, Andrés J, Safont VS (1995) J Mol Struct (Theochem) 342: 131
35. Andres J, Moliner V, Krechl J, Domingo JL, Picher MT (1995) J Am Chem Soc 117: 8807
36. Tapia O, Poulain E, Sussman F (1975) Chem Phys Lett 33: 65
37. Warshel A, Levitt H (1976) J Mol Biol 103: 227
38. Tapia O, Johannin G (1981) J Chem Phys 75: 3624
39. Singh UC, Kollman PA (1986) J Comput Chem 7: 718
40. Tapia O, Colonna F, Angyan JG (1990) J Chim Phys 87: 875
41. Tapia O (1992) J Math Chem 10: 139
42. Tomasi J, Persico M (1994) Chem Rev 94: 2027
43. Sehgal A, Shao L, Gao J (1995) J Am Chem Soc 117: 11337
44. Barnes JA, Williams IH (1996) J Chem Soc Chem Commun 193
45. Bash PA, Field MJ, Karplus M (1987) J Am Chem Soc 109: 8092
46. Field MJ, Bash PA, Karplus M (1990) J Comput Chem 11: 700
47. Bash PA, Field MJ, Davenport GA, Petsko D, Karplus M (1991) Biochemistry 30: 5826
48. Waszkowycz B, Hillier IH, Gensmantel N, Payling DW (1991) J Chem Soc, Perkin Trans 2: 225
49. Aqvist J, Warshel A (1993) Chem Rev 93: 2523
50. Lyne P, Mulholland AJ, Richards WG (1995) J Am Chem Soc 117: 11345
51. Barnes JA, Williams IH (1996) Biochem Soc Trans 24: 263
52. Moliner V, Turner AJ, Williams IH (1997) J Chem Soc Chem Commun 1271
53. Turner AJ (1997) University of Bath, Thesis
54. Lorimer GH, Gutteridge S, Madden MW (1987) In: Plant molecular biology. Plenum, New York, pp 21–31
55. Andrews TJ, Lorimer GH (1987) In: The biochemistry of plants. Academic, New York, pp 131–218
56. Hartman FC, Harpel MR (1994) Annu Rev Biochem 63: 197
57. Hartman FC (1992) In: Plant protein engineering. Cambridge University Press, Cambridge, pp 61–92
58. Saver BG, Knowles JR (1982) Biochemistry 21: 5398
59. Sue JM, Knowles JR (1982) Biochemistry 21: 5404
60. Hartman FC, Soper TS, Niyogi SK, Mural RJ, Foote RS, Mitra S, Lee EH, Machanoff R, Larimer WF (1987) J Biol Chem 262: 3496
61. Lorimer GH, Hartman FC (1988) J Biol Chem 263: 6468
62. Smith HB, Larimer FW, Hartman FC (1988) Biochem Biophys Res Commun 152: 579
63. Schloss JV (1990) In: Enzymatic and model carboxylation and reduction reactions for carbon dioxide utilization. Kluwer, Dordrecht, pp 321–345
64. Newman J, Gutteridge S (1993) J Biol Chem 268: 25876
65. Andersson I (1996) J Mol Biol 259: 160
66. Safont VS, Oliva M, Andres J, Tapia O (1997) Chem Phys Lett 278: 291
67. Tapia O, Andres J (1992) Mol Eng 2: 37
68. Andrés J, Safont VS, Tapia O (1992) Chem Phys Lett 198: 515
69. Andrés J, Safont VS, Queralt J, Tapia O (1993) J Phys Chem 97: 7888
70. Tapia O, Andrés J, Safont VS (1994) J Phys Chem 98: 4821
71. Tapia O, Andres J, Safont VS (1996) J Phys Chem 100: 8543
72. (a)Knight S, Andersson I, Bränden C (1990) J Mol Biol 215: 113; (b)Andersson I (1996) J Mol Biol 259: 160
73. Taylor TC, Andersson I (1996) Nat Struct Biol 3: 95
74. Taylor TC, Fothergill D, Andersson I (1996) J Biol Chem 271: 32894
75. Taylor TC, Andersson I (1997) Biochemistry 36: 4041
76. Taylor TC, Andersson I (1997) J Mol Biol 265: 432
77. Schlegel HB (1982) J Comput Chem 3: 214
78. Schlegel HB (1982) J Chem Phys 77: 3676
79. Frisch MJ, Trucks GW, Schlegel HB, Gill PMW, Johnson BG, Robb MA, Cheeseman JR, Keith T, Peterson GA, Montgomery JA, Raghavachari K, Al-Laham MA, Zakrzewski VG, Ortiz JV, Foresman JB, Cioslowski J, Stefanov BB, Nanayakkara A, Challacombe M, Peng CY, Ayala PY, Chen W, Wong MW, Andres JL, Replogle ES, Gomperts R, Martin RL, Fox DJ, Binkley JS, Defrees DJ, Baker J, Stewart JP, Head-Gordon M, Gonzalez C, Pople JA (1995) GAUSSIAN94, Revision B.1 Gaussian, Inc., Pittsburgh, Pa
80. Nakagawa S, Yu HA, Karplus M, Umeyama H (1993) Proteins 16: 172
81. Dewar MJS, Zoebisch EG, Healy EF, Stewart JJP (1985) J Am Chem Soc 107: 3902
82. Brooks BR, Bruccoleri RE, Olafson BD, States DJ, Swaminathan S, Karplus M (1983) J Comput Chem 4: 187
83. Tapia O, Andres J (1984) Chem Phys Lett 109: 471
84. Cleland WW, Andrews TJ, Gutteridge S, Hartman FC, Lorimer GH (1998) Chem Rev 98: 549
85. Pauling L (1948) Nature 161: 707
86. Fukui K (1970) J Phys Chem 74: 4161